



EXPERIMENTAL RESEARCH ON END JOINT OF STEEL-CONCRETE COMPOSITE TRUSS

Lingyu Zhou¹✉, Guichao He²

¹School of Civil Engineering, Central South University, Shaoshan south road, No. 22,
Changsha 410075, China

²AVIC APC Changsha Design and Research Co., Ltd, Xiangzhang Road, No. 254, Changsha 410014, China
E-mails: ¹zhoulingyu@csu.edu.cn; ²hgchao@csu.edu.cn

Abstract. Steel-concrete composite truss is characterized by such advantages: high stiffness, low height and construction costs. Moreover, it has promising application prospects. Since the interfacial load between concrete and steel is still indeterminate, experimental research and finite element analysis were carried out on two samples in scale of 1:3 models of composite truss joint models. A detailed account of the design philosophy, structural origin, loading procedure and test items followed. Test results showed that under design load, the joints were at elastic stage all along. Joints cracking load was twice as much as the design load. Their yield load was 3.2 times the design load and the ultimate load was 3.5 times the design load. The joints had a high safety factor which met the design requirements. The joints failing process was that cracks appeared on concrete first, and the web members yielded soon after, leading to joint yield. Now that both the concrete chord and the steel web members failed, there is no obvious increase in joint bearing capacity after joint yield. But the joints underwent severe deformation and possessed good ductility. For this reason, the joints could be applied in engineering practice.

Keywords: bridges, steel-concrete composite truss joint, ultimate bearing capacity, experimental research, finite element analysis.

1. Introduction and objective

Steel-concrete composite truss is a new type of structure developed in recent years. Since both the top and bottom chords are made of concrete which were adopted in various rail structures, consumption of steel in construction decreases sharply. In the meanwhile, the structure stiffness is stronger than that of steel truss girder. Furthermore, steel structures are applied in web members only, resulting in low maintenance and construction costs. In view of the above advantages, some researches have been carried out on this bridge type, and applied in engineering practice. A series of composite truss girder bridges have been constructed in France (Tanis 2003), Germany (Reis 2011), Switzerland (Dauner *et al.* 1998) and Japan (Hirohisa *et al.* 2001; Koyama 2003).

The composite joint is one of the most important parts for such a bridge structure. It is a key to develop a new joint construction and understand the behaviors of the joint. The joints should properly and effectively transfer force between different materials. From the practical perspective, there has been some experimental research on the alternative of an effective joint, thus various joints have been proposed and tested.

Udomworarat *et al.* (2000; 2002) studied the fatigue performance and ultimate strength of welded steel tubular joints. Sakai *et al.* (2004) conducted an experimental study on the ultimate strength and fatigue strength of concrete filled and additionally the reinforced tubular K-joint of truss girders. Toshio *et al.* (2004) proposed a new type of joint that has the outer tubes welded to steel plates outside the steel trusses in the concrete slabs. Static loading tests were carried out to verify the strengthening performance. Kosuke *et al.* (2006) introduced various junction structures and explained their features. Furthermore, some experiments and analyses were carried out concerning the design method of the new joint structures which the authors devised. Sato *et al.* (2008) proposed two kinds of joint structures with perfobond shear connectors and welded headed studs. The loading test in half scale specimens of the joint structure has been carried out to clarify the stress transfer mechanism of the joint structure. Hino *et al.* (1985) performed bending tests on steel-PSC beams and steel-reinforced concrete beams with three types of mechanical joints: anchor bars, studs, and bolts. Dunai (2004) investigated the behavior of end-plate-type steel-to-concrete connections with bolts and studs under

combined compressive axial forces and cyclic bending moments. The composite truss concept has been applied to large-span bridges such as railway bridges. Experimental researches have only been carried out (Kim *et al.* 2011; Takashi *et al.* 2002; Toshio *et al.* 2005; Xue *et al.* 2011) on certain composite truss bridges.

In 2009, steel-concrete composite truss was used in Xi'an-Pingliang Railway. Intensive research has been carried out. The top chord joint at the composite truss support bears the maximal unbalanced horizontal thrust from the top concrete chord near the supports, as shown in Fig. 1. The composite truss joint consists of diagonal steel web members and concrete chords. How to ensure that the shear is distributed between concrete and steel plate remains the key technical problem.

This plan features the PBLconnectors (Valente, Cruz 2004; Vianna *et al.* 2009) bearing the shearing and bending moment. This innovative composite truss structure was initially used in China, which needs experimental and numerical analysis to fully understand



Fig. 1. Steel structure of composite truss bridge

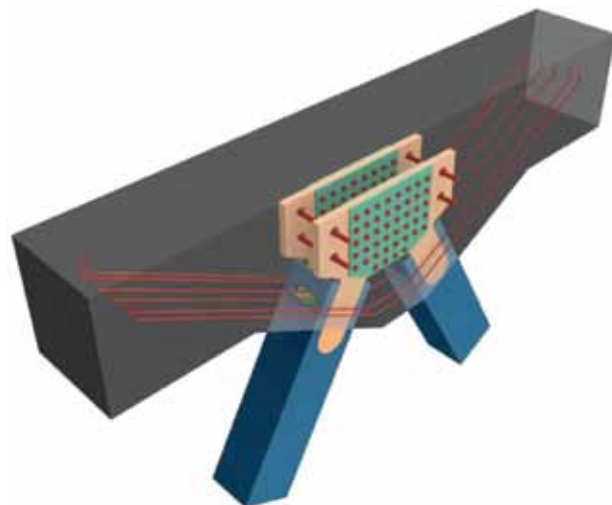


Fig. 2. Structure of joint

the safety and serviceability. Although some composite truss bridges have been constructed, theoretical and experimental researches are rare for this kind of joints in bridges. Major shortcoming of these researches lies in that no joint model test is carried out yet. 1:3 models of joints are designed and tested at Central South University to evaluate working performance, failure modes and ultimate bearing capacity of such joints.

2. Joint model

2.1. Introduction to prototype joint

Houhecun Bridge, Mawujing Bridge and Taiyu Bridge on Xi'an-Pingliang Railway all have a same span of 80 m adopting steel-concrete composite truss, as shown in Fig. 1. The main truss is a triangle truss of 9 m in height with no montant. The joint length is 10 m. For the top chord, a rectangular cross section of steel concrete is adopted which is 1.1 m in width and 1.2 m in height. The bottom chord adopts a channel cross section with a beam height of 1.5 m, and the beam end is 2.0 m thick. In the longitudinal direction there is a fully prestressed structure and in the lateral there is reinforced concrete structure. Rectangular steel box of 550×650 (mm) is used for web members with a wall thickness of 24 mm.

2.2. Joint model design

The end joint of top chord of composite truss (Fig. 1) bears the max unbalanced horizontal load. Because the mechanical behavior and deformation of concrete and steel are different, the mechanical behavior of joints becomes quite complicated. In order to ensure that the joints have a reasonable bearing capacity and a safe and reliable structure, a structure plan is proposed, as shown in Fig. 2. The chord wraps up almost all the joint plate in its enlarged cross section. Holes are drilled on the joint plate to assure strength of the bond between the concrete and the plate. Strengthened reinforcements run through the holes at the end of joint plate to form PBL shear connectors which bear the load transmitted from the chord. Web members are welded onto both ends of the joint plate to bear tensile and compressive loads.

Experimental research is carried out to better understand the ultimate bearing capacity and stiffness of joints, the stress and its distribution on the interface between steel and concrete, as well as the relationships between load and stress, load and strain, and the development tendency of concrete cracks. This bridge has to bear China Railway standard middle-live loading. In regard to the structure of single-track composite truss bridge, the max force is about 9000 kN. To meet the requirements for testing devices, two 1:3 joint models ZHJD-1 and ZHJD-2 are produced. The design load is taken as 1000 kN. Web members and joint plates of the specimens are made of steel Q345. The chord is made of concrete C50 and reinforcement HRB335. Detailed joint structure and its geometric size are shown in Fig. 3.

3. Testing process

3.1. Test configuration and loading

The ground anchored groove and reaction wall system in the *Laboratory of Safety Science of Civil Engineering at Central South University* are adopted for loading purpose. Joint specimen is installed onto the loading base on one side of the reaction wall. One end of the 5000 kN jack is set against the reaction wall while the other end is against the concrete chord. Horizontal force is exercised on joint specimen. In order to ensure axial movement of the specimen in loading process, vertical bracing and lateral pulley device are provided on both ends of the chord. Loading device of joint model is shown in Fig. 4.

Before test, preloading is adopted to make sure all instruments work normally. When formal loading begins, load control is used. When the load is between 0~2 000 kN, its loading level is 400 kN. When the load is between 2000 kN~3 000 kN, its loading level is 200 kN. When the load is increased to above 3000 kN, the loading level is 100 kN.

3.2. Test items

Strain and displacement data in this test are collected by means of strain gauge and dialgauge as shown in Fig. 5. Rectangular rosettes are provided on the concrete of the chord, the joint plate and web members. Horizontal strain gauges are arranged on other parts of the chord. Once the load is increased by one loading level which lasts for 2 min, the static strain data acquisition instrument will start to collect data. The displacement gauging points and arrangement of strain gauges are completely the same for the two specimens.

4. Mechanical properties of materials

Specimen chord in the test is made of commercial concrete with a grade of C50. China Railway Turnout Bridge Inc. is entrusted to produce the steel structure of the specimen using Q345B steel. HRB335-grade reinforcements are used to produce the specimen. Mechanical properties of materials are shown in Table 1.

Table 1. Mechanical properties of materials

Member	Modulus of elasticity, GPa	Yield strength, MPa	Ultimate strength, MPa
Chord	35.2	–	54
Joint plate	203	390	565
Connection plate	206	375	535
Web member	205	380	540
Φ10	202	392.4	465.8
Φ16	198	397.1	540.1
Φ25	199	451.4	620.2

Note: all values are the average values of testing samples.

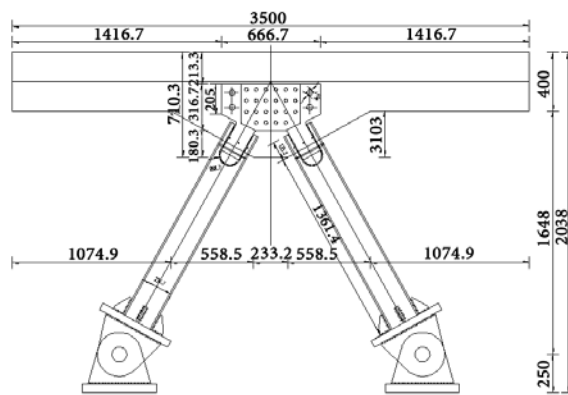


Fig. 3. Joint model structure and size, mm

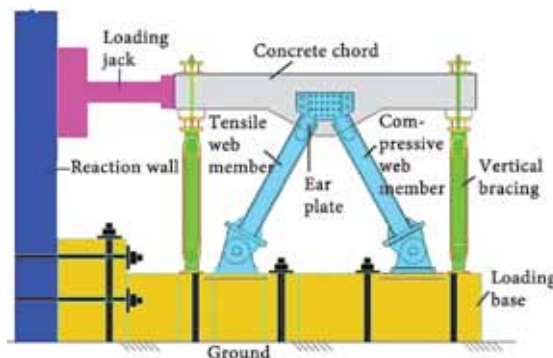


Fig. 4. Test loading device and specimen

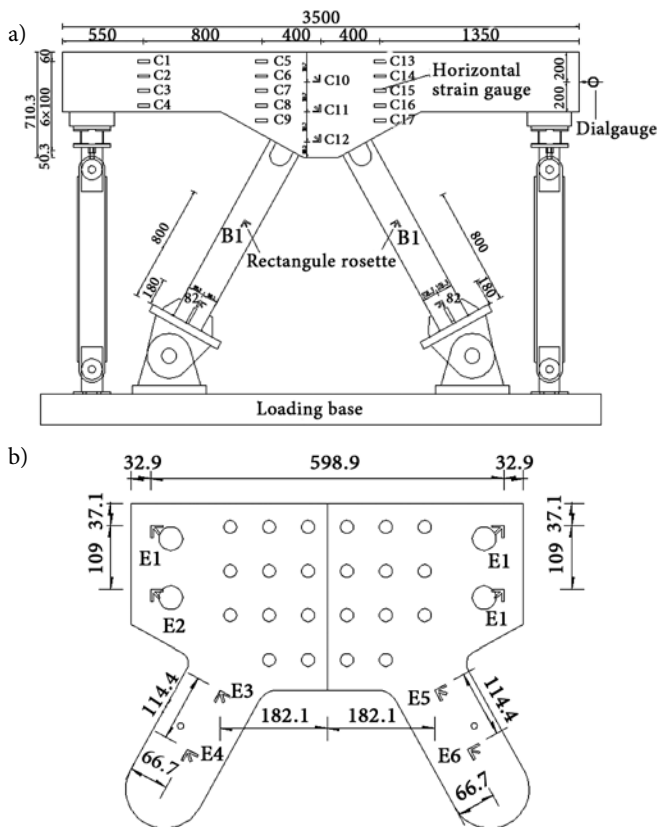


Fig. 5. Layout of joint displacement and strain gauging points (measurements in mm): a – front view of gauges on chord and web members; b – arrangement of gauging points on joint plate

5. Test results

5.1. Description

When 1600 kN is loaded onto ZHJD-1, the strain and the displacement grow evenly. The strain of each point is smaller than the material yield strain. No concrete cracking and steel buckling were found. In the process when the

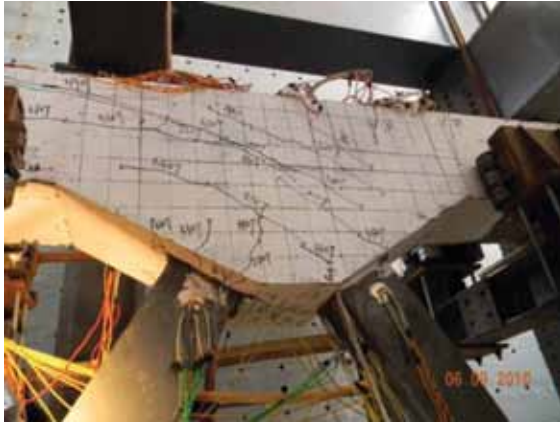


Fig. 6. Distribution of ZHJD-1 concrete cracks $P = 3800$ kN



Fig. 7. Buckling of ZHJD-1 compressive web member $P = 3800$ kN

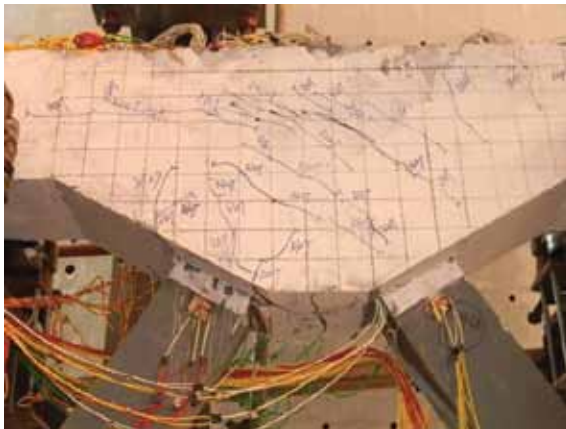


Fig. 8. Distribution of cracks on ZHJD-2 concrete surface $P = 3500$ kN

load is increased to 2000 kN, cracks are seen on concrete for the first time, mainly on the enlarged cross section, between two web members and at the sectional corner of the compressive web member. Cracks develop in the direction which has an included angle of 40° with the axial direction of the chord. When the loading level grows, many new cracks appear on the concrete surface in the same direction. The locations and development tendency of cracks are the same on both sides. When the load is increased to 2800 kN, cracks appear on concrete at the sectional corner of the tensile web member, which join in the cracks on concrete surface. When the load is increased to 3200 kN, cracks on concrete surface develop horizontally towards the loading end. When the load is between 3600 kN and 3700 kN, horizontal cracks develop very fast. At the same time, two vertical cracks appear on free end of the chord which run the length of the chord. Cracks on concrete surface are shown in Fig. 6.

When the load is smaller than 3300 kN, strains of gauging points on tensile and compressive web members grow evenly, indicating that the web members are in elastic stage. When the load keeps increasing, nothing abnormal happens to the web members. But strains of the gauging points grow fast, showing that the material begins to yield. When the load is increased to 3800 kN, strains of the gauging points grow even faster. Bulking and concaves are observed on top of the compressive web member. The loading comes to a stop when the compressive web member experiences severe deformation. The tensile web member experiences no failure. Local buckling of the compressive web member is shown in Fig. 7.

In ZHJD-2, before the load is increased to 3200 kN, strains of gauging points on tensile and compressive web members grow evenly, and the web members perform normally. When the load keeps increasing to 3500 kN, no failure is seen on both web members, but the strains of the gauging points increase quickly, indicating that the web members are in elasto-plastic stage. And the cracking in the chord keeps on developing, shown in Fig. 8. When the load is increased to between 3500 kN and 3600 kN strains of the gauging points increase dramatically. Bulking and concaves are found on steel plates on top of the compressive web member. The steel plate in the inner side of the lower part of the compressive web member experiences tearing failure. It deforms severely. The loading comes to a stop. No macroscopical failure are found seen on the tensile web member. Local buckling of the compressive web member is shown in Fig. 9.

From the above, the stiffness of the two joints changes evenly at the steel-concrete interface. No mutation is found in stress distribution of steel-concrete interface, indicating a good mechanical behavior of the faying face and even transmission of the load. Steel and concrete experience small slips (both vertical and longitudinal). Failure of the model is not under control of the interface. The joints possess good shearing stiffness and strength. It is feasible to connect the steel and the concrete with PBL shear connectors in composite truss joints.

5.2. Load-displacement curves

Fig. 10 indicates the respective load-horizontal displacement curves of the free ends of chords ZHJD-1 and ZHJD-2. The load-horizontal displacement curve of ZHJD-1 is quite plump with no obvious turning point. Before the load is increased to 3200 kN, displacement grows following load increase. Though cracks appear at 2000 kN, no turning point appear in the curve. The slope remains unchanged at this moment, concrete cracking has so little influence on joint stiffness. The joints undergo no stiffness degradation. When the load is increased to over 3200 kN, slope of the curve decrease gradually until it becomes level. Reasons are that the web member material starts to yield at 3200 kN, leading first to severe deformation and then stiffness degradation of both joints. It shows that web members have great influence on mechanical properties of joints. Joints deform severely after yielding, with good ductility, but with no brittle failure.

The load-horizontal displacement curve of ZHJD-2 shows similar development tendency with that of ZHJD-1. But the curve of ZHJD-2 is not plump because there is an obvious turning point in it. Its ultimate failing load is 3500 kN, which is lower than that of ZHJD-1, but with larger displacement. On the whole, the bearing capacities of both joints are greater than the design load of 1000 kN. With high safety factor and sufficient bearing capacity, the joints meet the design requirements and will be applied in engineering practice.

Table 2 shows the characteristic loads of the two joints obtained from their respective load-displacement curves, which are then compared with the design load. The joints have sufficient bearing capacities which meet the design requirements. Their cracking loads are twice that of their design load.

5.3. Load-strain curves

From the joint failure modes, the two specimens undergo the same failures, which justifies the analysis of strain test results of specimen ZHJD-2.

Fig. 11 shows the load-axial strain measured curves of the gauging points of the concrete. When concrete of the gauging points in the 1st column is under axial load, strains at each gauging point are all compressive ones. Even though the figures are a bit different at the early loading stage, the differences are not significant at all. No crack is seen here. The strains experience linear growth following load increase. There is no obvious turning point in the curves.

Gauging points in the 2nd column are at the enlarged cross section where the concrete is close to the tensile web member, under whose influence, gauging points C8 and C9 experience tensile strain at the very beginning of loading. Before the load is increased to 2000 kN, the strain sees linear growth. While under the influence of concrete cracking, the stiffness of the curve decreases a little, but is still in linear growth. When the load is increased to 3000 kN, cracks appear at the gauging points. The tensile strain grows very fast, while slope of the curve drops sharply. The measured tensile strain of the gauging points



Fig. 9. Failure of ZHJD-2 compressive web member P = 3500 kN

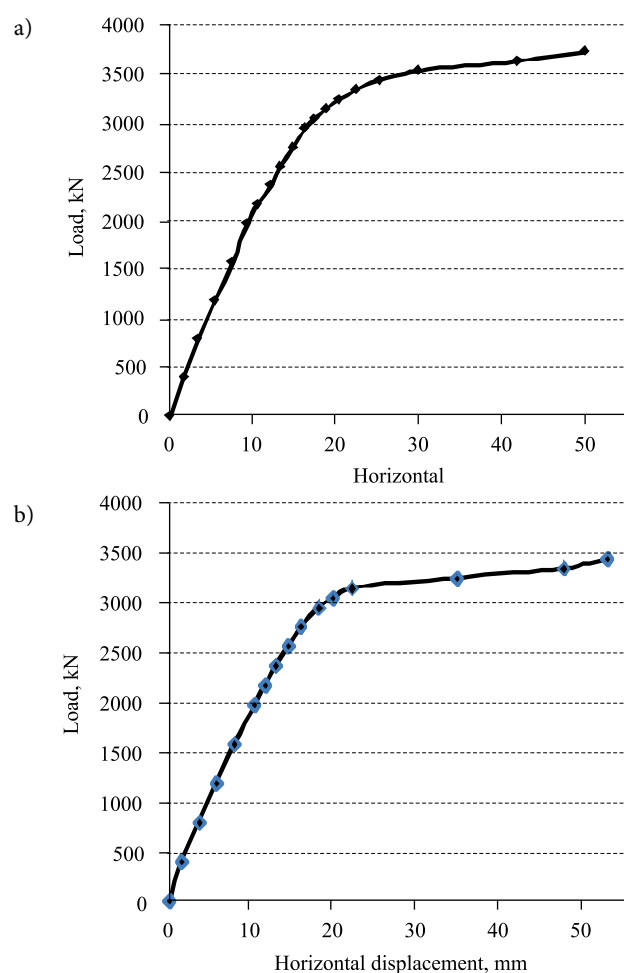


Fig. 10. Load-horizontal displacement curves of the free ends of chords: a – ZHJD-1; b – ZHJD-2

Table 2. Joint test

Type of joints	Characteristic load					
	Cracking load, kN	Ratio to design load, kN	Yield load, kN	Ratio to design load, kN	Ultimate load, kN	Ratio to design load, kN
ZHJD-1	2000	2.0	3300	3.3	3700	3.7
ZHJD-2	2000	2.0	3000	3.0	3500	3.5

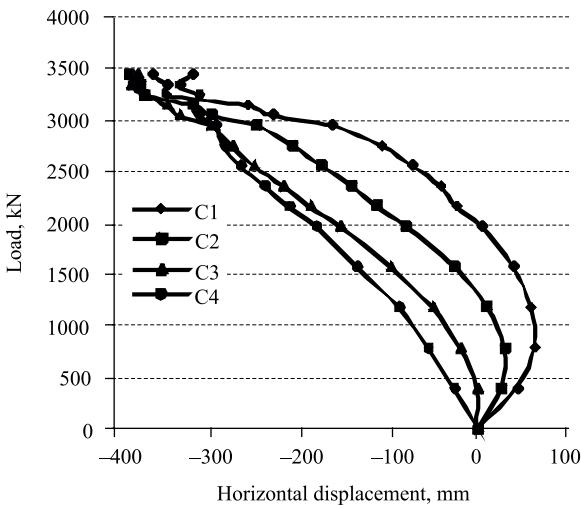
is far greater than the ultimate tensile strain of the concrete. Gauging points C5 and C6 are in compression on the top of the chord. Being far from the joint, they are affected little by concrete cracking. Slope of their curves changes less than those of C8 and C9. When the tensile web member yields, the curves turn sharply.

Gauging points in the 3rd column are at the center of the enlarged cross section. At the early loading stage, the strain is small. Following increase of the load, the tensile stress of the concrete under the bending-shearing function exceeds the ultimate tensile strength. At this moment, cracks appear on the concrete and the strain grows rapidly. When the load is increased to 3200 kN, under the influence of web member yield, the curve turns and the strain keeps growing. Strain of gauging point C12 decreases abruptly at the later loading stage, showing that the cracks go beyond the strain gauge.

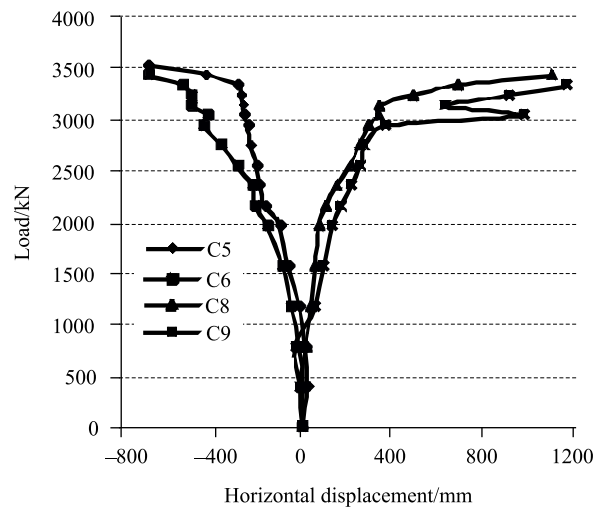
Gauging points in the 4th column are also at the enlarged cross section. Most of the load is distributed to the

web members through the joint plate. The strains of these points are smaller than those of the gauging points in previous three columns. From Fig. 11, small strains are in linear growth. Under the influence of stress concentration at the sectional corner of the compressive web member, one of the gauging points undergoes tensile stress, which develops very fast. When cracks go beyond this gauging point the tensile stress increases quickly.

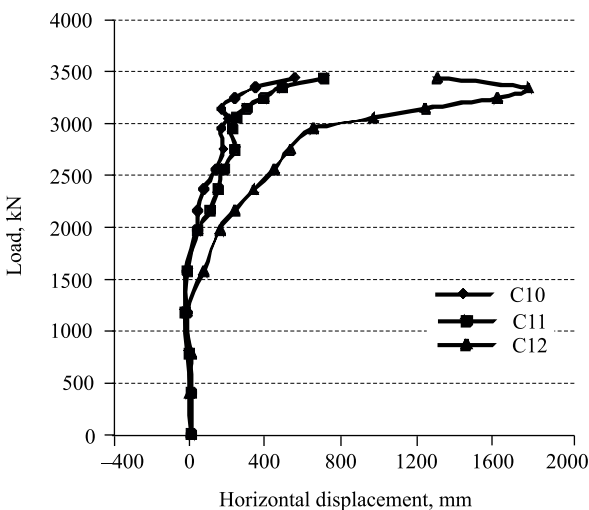
Fig. 12 shows the load-axial strain curves of the tensile and compressive web members. At the early loading stage, load and strain are in linear relation. When the joints are under load, the chord rotates a little. In addition to the axial load, the web members have to bear part of the additional bending moment, therefore strains of each point differ a little. But the difference is not big, showing that additional bending moment is small, and the web members bear mainly the axial tensile and compressive loads. A turning point is on the strain curve of the tensile web member joint when the load is 3300 kN, showing that



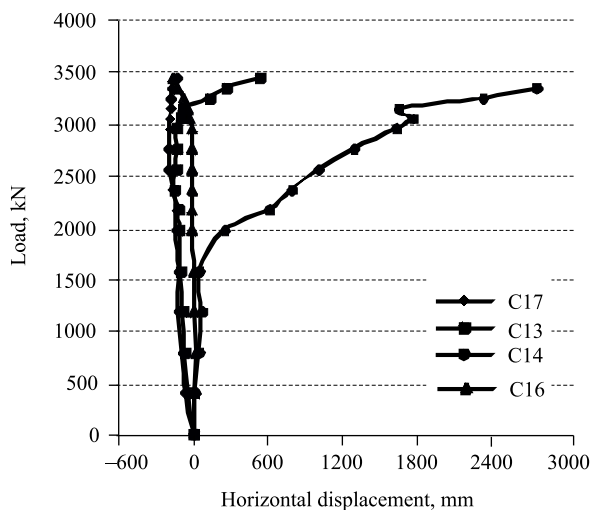
a) 1st column



b) 2nd column



c) 3rd column



d) 4th column

Fig. 11. Concrete strain test results

this web member reaches its material yield strength. The joint begins to yield, the curves change horizontally, and the joint bearing capacity grows slowly. At the same time, the strains increase quickly. The compressive web member yields under a load of 3200 kN. The strain decreases quickly afterwards to nearly zero when loading stops. The reason is that at the later loading stage, local buckling occurs on the compressive web member. Its lower part is under load, the steel plate at the sectional corner is torn. The two gauging points are within the failing part.

5.4. Joint failure modes

According to the testing process, the concrete failures of the two joints are almost the same: 40 diagonal cracks are on concrete surface at the sectional corner of the chord. Cracks at the chord axis stretch upwards till they become level. While cracks under the joint extend downwards till they arrive at the compressive web member. In the meanwhile, since the web members are of box beam cross section, stress concentration appears at the corner. Cracks are on the concrete nearby. They appear on concrete at the compressive web member early than at the tensile web member. Cracks nearby the compressive web member are shorter and develop more slowly.

Macroscopical failure is not seen on the tensile web member. Local buckling appears on the compressive web member. Bulking and concaves are seen on the steel plates nearby the concrete with so large an area that it is almost the height of the web member. In addition, the steel plate inside the bottom of the compressive web member of ZHJD-2 is torn.

There are three types of failures for joint plate joints, i.e., diagonal cracking of concrete on the joint surface, concrete cracking at the sectional corner of both web members, and the buckling failure of the compressive web member.

6. Finite element analysis

Finite element analysis software ANSYS is adopted for analysis of the joints. The geometric size of the finite element model (FEM) is the same as that of the specimen size. Elastic-plastic shell element SHELL8 is used to simulate the support and the steel web member. Solid element SOLID65 is used to simulate the concrete chord. Solid element SOLID45 is used to simulate the joint plate and the shear reinforcement. The 3 dimension bar element LINK8 is used to simulate reinforcement in concrete. Willam-Warnke five parameters failure criteria are adopted for concrete. Material properties are determined according to the properties test results. Suppose all materials are ideal ones in conformance with Mises yield criterion, Newton-Raphson iteration method is used to find out the solution. At the same time, material non-linearity and geometrical non-linearity are considered. Since the test results indicate no failure through steel-to-concrete contact, the perfect connection between concrete and joint plate was adopted in the FEM, as shown in Fig. 13.

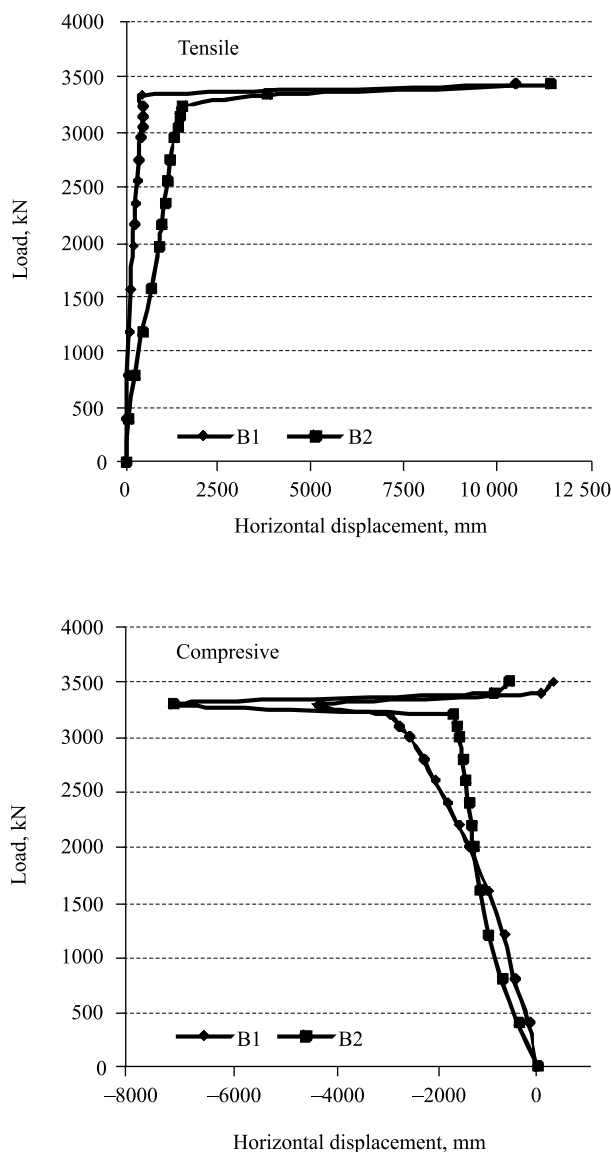


Fig. 12. Web member strain test results



Fig. 13. FEM and mesh

Fig. 14 presents Mises stress distribution (under a load of 3500 kN) of the steel member. There is obvious stress concentration at the corner inside the joint plate of the tensile web member. The max stress exceeds the yield stress of the material. Other than being buried in concrete, the rest of the two web members are yielded, with a maximum stress of 386.2 MPa. The calculation results agree with the test results.

Fig. 15 shows the measured and the calculated load-displacement curves of the free end of the chord, from which the finite element analysis results are in good agreement with the measured results, except that the calculated yield point is a bit high. When at the yield point, the load will not be increased and the joint stiffness will decrease till it is zero. Because it is related to the constitutive

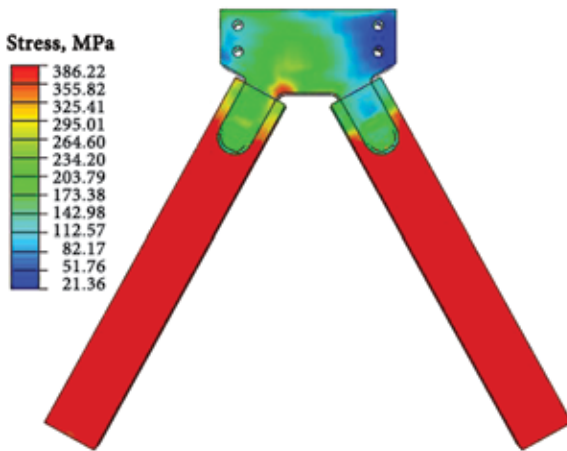


Fig. 14. Mises color stress cloud chart of steel member
P = 3500 kN

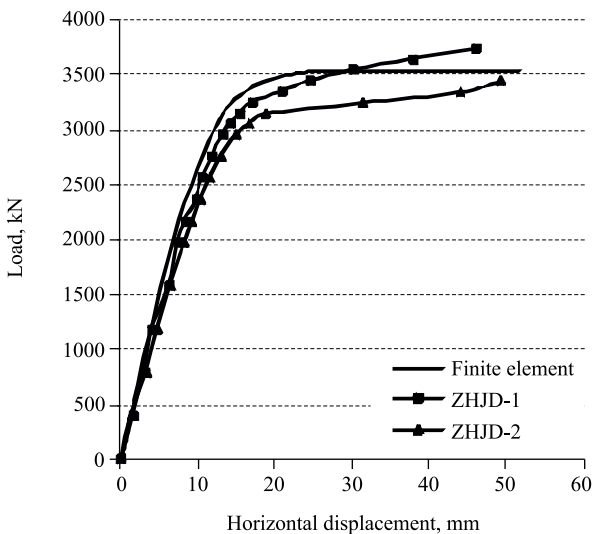


Fig. 15. Comparison of load-displacement curves of joints

relation of the materials, and no complete simulation is achieved using finite element analysis method.

According to the test results and the finite element analysis results, 1:3 model joint cracking load is 2000 kN, which is twice the design load. Its yield load is 3200 kN, which is 3.2 times the design load. The ultimate load is 3500 kN, 3.5 times the design load. High safety performance is ensured. The developed FEM is used simulating behavior of the joint.

7. Conclusions

Based on the three bridges on Xi'an-Pingliang Railway, a new structure – steel-concrete composite truss structure is proposed according to its construction characteristics. Now that the interfacial load between steel and concrete is complicated, experimental research and finite element analysis are performed on joint plate joints. The following conclusions are drawn:

1. According to the test results and the finite element analysis results, it is safe for the joints to bear the load of bridge. The cracking load is twice the design load. The yield load is 3.2 times the design load. The ultimate load is 3.5 times the design load. The joints enjoy high security reserve and sufficient bearing capacity. The cracking load is 57% of the ultimate load, while the yield load is 92% of the ultimate load. The joints reach their ultimate value soon after they yield, experiencing severe deformation and possessing good ductility.

2. The finite element calculation values of the load-horizontal displacement curves of the free end of the chord are in good agreement with the measured values. Finite element is used for analysis and calculation of the joints.

3. There are three types of failures for joint plate joints, i.e., diagonal cracking of concrete on the enlarged cross section of the chord joint, concrete cracking at the sectional corner of both web members, and local buckling on the top and bottom of compressive web members.

4. Cracks distribute mainly on the surface of the chord joint, forming an included angle of 40° with the axial direction of the chord. The joint plate is buried in concrete, with good mechanical behaviors and there is nothing abnormal. Local buckling appears on the compressive web member, leading to final failure of joints.

Acknowledgement

This project is financially supported by Department of Science and Technology MOR(2008G007-C) and National Natural Science Foundation of China(50708112). The research is supported by China Railway First Survey and Design Institute. The Laboratory of Safety Science of Civil Engineering at Central South University provides with the testing sites and loading instrument. And thank the nameless conscientious reviewers for the professional comments. To them the authors want to express their appreciation.

References

- Dauner, H. G.; Oribasi, A.; Wéry, D. 1998. The Lully Viaduct-A Composite Bridge with Steel Tube Truss, *Journal of Constructional Steel Research* 46(1–3): 67–68. [http://dx.doi.org/10.1016/S0143-974X\(98\)00025-X](http://dx.doi.org/10.1016/S0143-974X(98)00025-X)
- Dunai, L. 2004. Experimental and Numerical Studies on the Cyclic Behavior of Steel and Composite Joints, *International Journal of Steel Structures* 4(4): 197–208.
- Hino, S.; Hamada, S.; Kaneyuki, K.; Hasegawa, H.; Nakano, H. 1985. Flexural Behavior of Mixed Steel-Concrete Beams with Various Joints, *Memoirs of the Faculty of Engineering* 35(2): 291–299.
- Hirohisa, N.; Hidekazu, N.; Hideki, N.; Hiroyoshi, N. 2001. Design of a Steel/Concrete Composite Truss Bridge, *Miyaji Technical Report* 17: 4–19.
- Kosuke, F.; Yoshihiro, H.; Kentaro, Y.; Tomoaki, H.; Masato, Y.; Hiroo, M. 2006. The Proposal of a Design Method of the Joint Structure for the Steel/Concrete Truss Bridge, *Doboku Gakkai Ronbunshuu F* 62(2): 349–366. <http://dx.doi.org/10.2208/jscejf.62.349>
- Koyama, S. 2003. Design and Construction of Itabashigawa Bridge, *Japanese Bridge and Foundation Engineering* 4: 43–56.
- Kim, S.-H.; Lee, Ch.-G.; Kim, S.-J.; Won, J.-H. 2011. Experimental Study on Joint of Spliced Steel-PSC Hybrid Girder, Part II: Full-Scale Test of Spliced Hybrid I-girder, *Engineering Structures* 33(9): 2668–2682. <http://dx.doi.org/10.1016/j.engstruct.2011.05.016>
- Reis, A.; Oliveira, P.; José, J. 2011. Composite Truss Bridges: New Trends, Design and Research, *Steel Construction* 4(3): 176–182. <http://dx.doi.org/10.1002/stco.201110024>
- Sakai, Y.; Hosaka, T.; Iseo, A.; Ichikawa, A.; Mitsuki, K. 2004. Experiments on Concrete Filled and Reinforced Tubular K-Joints of Truss Girder, *Journal of Constructional Steel Research* 60(3–5): 683–699. [http://dx.doi.org/10.1016/S0143-974X\(03\)00136-6](http://dx.doi.org/10.1016/S0143-974X(03)00136-6).
- Sato, Y.; Hino, S.; Yoshimi, S. 2008. Study on Load Transfer Mechanism of the Joint in Hybrid Truss Bridge, *Journal of Structural Engineering A ASCE* 54: 778–785.
- Tanis, J.-M. 2003. Bras de la Plaine Bridge, Reunion Island, France, *Structural Engineering International* 13(4): 259–262. <http://dx.doi.org/10.2749/101686603777964388>
- Toshio, N.; Satoru, O.; Toshiaki, K. 2005. *Study on Strengthening Performance of Joints in PC Hybrid Truss Bridges (Part 2) – Static Loading Test with 1/2-Scale Model Specimen*. Obayashi Corporation Technical Research Report. Japan: Obayashi Corporation Technical Research Institute. 69 p.
- Toshio, N.; Satoru, O.; Toshiaki, K. 2004. *A Study on Structural Performance of Joint in PC Hybrid Truss Bridge*. Report of Obayashi Corporation Technical Research Institute. Japan: Obayashi Corporation Technical Research Institute. 25 p.
- Udomworarat, P.; Miki, C.; Ichikawa, A.; Komechi, M.; Mitsuki, K.; Hosaka, T. 2002. Fatigue Performance of Composite Tubular K-joints for Truss Type Bridge, *Structural Engineering/ Earthquake Engineering* 19(2): 65S–79S.
- Udomworarat, P.; Miki, C.; Ichikawa, A.; Sasaki, E.; Sakamoto, T.; Mitsuki, K.; Hosaka, T. 2000. Fatigue and Ultimate Strengths of Concrete Filled Tubular K-joints on Truss Girder, *Journal of Structural Engineering* 46A(3): 1627–1635.
- Valente, I.; Cruz, P. J. S. 2004. Experimental Analysis of Perfbond Shear Connection between Steel and Lightweight Concrete, *Journal of Constructional Steel Research* 60(3–5): 465–479. [http://dx.doi.org/10.1016/S0143-974X\(03\)00124-X](http://dx.doi.org/10.1016/S0143-974X(03)00124-X)
- Vianna, J. da. C.; Costa-Neves, L. F.; Vellasco, P. C. G. da S.; de Andrade, S. A. L. 2009. Experimental Assessment of Perfbond and T-Perfbond Shear Connectors' Structural Response, *Journal of Constructional Steel Research* 65(2): 408–421. <http://dx.doi.org/10.1016/j.jcsr.2008.02.011>
- Xue, D.; Liu, Y.; He, J.; Ma, B. 2011. Experimental Study and Numerical Analysis of a Composite Truss Joint, *Journal of Constructional Steel Research* 67(6): 957–964. <http://dx.doi.org/10.1016/j.jcsr.2011.01.013>

Received 29 November 2011; accepted 7 February 2012